Journal of Quantitative Spectroscopy & Radiative Transfer 222–223 (2019) 122–129

Contents lists available at ScienceDirect

Journal of Quantitative Spectroscopy & Radiative Transfer

journal homepage: www.elsevier.com/locate/jqsrt

Measurement of the mid-infrared absorption spectra of ethylene (C_2H_4) and other molecules at high temperatures and pressures

C.L. Strand*, Y. Ding, S.E. Johnson, R.K. Hanson

High Temperature Gasdynamics Laboratory, Thermosciences Division, Stanford University, 452 Escondido Mall, Bldg. 520, Stanford, CA 94305, USA

ARTICLE INFO

Article history:
Received 23 July 2018
Revised 18 September 2018
Accepted 18 October 2018
Available online 19 October 2018

ABSTRACT

A methodology for the measurement of mid-infrared absorption cross sections of gaseous molecules at high temperatures and pressures is presented. A rapid-tuning, broad-scan external cavity quantum cascade laser with a tuning rate in excess of 30000 $cm^{-1}s^{-1}$ has been employed in the measurement of full vibrational bands (> 100 cm^{-1}) in shock-heated test gases. The approach is demonstrated with measurements of the absorption cross section of ethylene (C_2H_4) in the 8.5 μm to 11.7 μm region for temperatures from 8.0 to 1.00 K and pressures from 1 to 5 atm. Decreasing peak strength with temperature is observed as well as pressure-insensitivity. The measurements are compared with existing experimental, empirical, and *ab initio* databases. Additionally, illustrative absorption cross section measurements of propene (C_3H_6), 1-butene (1-C_4H_8), 2-butene (2-C_4H_8), 1,3-butadiene (1,3-C_4H_6), and methanol (CH_3OH) are presented near 1000 K and 2.3 atm.

© 2018 Elsevier Ltd. All rights reserved.

1. Introduction

There exists a marked lack of experimental absorption spectra for high-temperature and high-pressure gaseous molecules. Gases in these high-enthalpy thermodynamic states are present in a wide range of natural and man-made environments, such as cool stars, exoplanets, plasmas, explosions, flames, volcanoes, forest fires, combustion systems, hypersonic flows, industrial processes, and exhaust stacks. Correspondingly, these gases are the subject of scientific study and engineering employ for many fields, including astrophysics, environmental science, plasma physics, combustion science, aerospace engineering, chemical engineering, and energy systems engineering. In the endeavor to study and monitor high-temperature gases, infrared absorption and emission spectroscopy offer a powerful toolset for understanding the characteristics of these environments [1–7]. This work presents a methodology using shock tube facilities in conjunction with rapid-tuning, broad-scan, narrow-linewidth lasers to measure the high-temperature and high-pressure absorption spectra of molecules in the mid-infrared.

Several databases exist to collate the infrared spectra and spectroscopic parameters of gaseous molecules. The most comprehensive and prominent line parameter and cross section databases, such as HITRAN, GEISA, PNNL Northwest Infrared, and NIST Quantitative Infrared Database, focus on molecules at or near room temperature and atmospheric pressures [8–11] . Additionally, there are a few databases, including HITEMP and ExoMol, that provide high-temperature spectral data but only for a limited subset of molecules [1,3].

The limited availability of high-temperature and high-pressure absorption and emission spectra stem primarily from the considerable challenges these conditions pose for *ab initio*, empirical, and experimental methods. High temperatures require the consideration of hot lines that emerge due to the population of higher energy levels, including high-J rovibrational transitions and vibrational hot bands. As a consequence, the number of lines that must be considered for accurate spectral modeling at high temperatures often increases by several orders of magnitude [1,2,12]. This issue is further compounded by increasing molecular size and correspondingly the number of vibrational modes, leading to the number of infrared lines for a single gas species to count in the billions.

Due to the weakness of hot lines at low temperatures and practical database considerations, hot lines are not typically observed, calculated, nor included in experimental, empirical, and *ab initio* room-temperature databases. This makes it impossible to accurately extrapolate room-temperature spectroscopic data to higher temperatures [2].

There are presently several initiatives to calculate, measure, and collate absorption spectra at high temperatures, including the two predominant databases HITEMP and ExoMol [1,3,13]. Unfortunately, the experimental validation is often quite limited, especially for larger molecules. This lack of experimental validation is primarily

* Corresponding author.
E-mail address: cstrand@stanford.edu (C.L. Strand).

https://doi.org/10.1016/j.jqsrt.2018.10.030
0022-4073/© 2018 Elsevier Ltd. All rights reserved.

the result of the same challenges that make any experimentation at high-temperature, high-pressure conditions difficult; namely the challenge of generating a well-known, homogeneous, chemically-stable, high-enthalpy gas state that remains steady for a sufficient duration to perform the desired experiment. All laboratory approaches achieve only a subset of these desired characteristics and must compromise on some to faithfully maintain the others. Moreover, the requirement of a stable chemical composition generally imposes an unavoidable upper-bound on the duration of the experiment. At elevated temperatures, accelerated reaction rates limit the experimental test time available to any experimental approach (e.g., the thermal decomposition of large molecules).

Standard approaches for achieving high-enthalpy conditions include radiative/conductive heating, rapid-compression, arc-heating, and shock-heating. With the exception of shock-heating, these approaches generally provide extended high-temperature test durations (from 100 ms up to several minutes) at the expense of stable chemical composition, temperature uniformity, or thermodynamic equilibrium, respectively. Shock-heating provides a near-ideal mechanism for instantaneously achieving a well-known, homogeneous, high-temperature and high-pressure environment with maximum temperatures and pressures in excess of 10000 K and 1000 atm, respectively. There is unfortunately the significant caveat of a very short test time (typically 1 to 10 ms but up to 100 ms is possible) in facilities that employ this mechanism, such as shock tubes.

In addition to the challenges of generating the desired conditions in a laboratory, the experimental challenges are further increased for the collection of spectroscopic reference data under these circumstances. This is due both to the characteristics of molecular spectra at high temperatures/pressures and the performance of the tools used to acquire spectra. High temperatures and high pressures lead to significant line broadening. The outcome of these broadening effects, in concert with the emergence of hot lines, is highly congested and blended spectra; wherein, individual lines are typically not observable and the local absorption or emission intensity is the result of the superposition of many neighboring lines. At these extreme conditions, the most practical parameterization of experimental spectroscopic measurements for both the interpretation of observed spectra and the validation of spectroscopic models is the wavelength-dependent absorption cross section over full absorption bands. Unfortunately, standard spectroscopic equipment such as spectrometers, FTIRs, and narrow-linewidth lasers generally provide a slow rate of acquisition for broad spectra and thus demand a laboratory approach to high-enthalpy conditions that emphasizes experimental duration at the cost of thermodynamic condition accuracy and range.

The recent development of rapid-tuning, broad-scan, narrow-linewidth lasers in the mid-infrared has enabled, for the first time, the practical use of a shock tube to perform quantitative broadband absorption spectroscopy measurements. Through tuning rates in excess of 30000 $cm^{-1}s^{-1}$, it has become possible to acquire the high-temperature absorption cross section over entire branches, or even entire bands, of large molecules during the short-duration steady test time of a shock tube.

2. Experimental methods

2.1. Shock tube

The experiments in this work were performed in a pressure-driven, high-purity, stainless steel shock tube with an inner diameter of 14.13 cm [14,15]. The shock tube consists of a 7.12 m high-pressure driver section followed by a 8.54 m low-pressure driven section that are separated by a polycarbonate diaphragm. The post-reflected shock conditions are determined using shock jump relations, assuming frozen chemistry. The necessary inputs are provided by the known initial driver gas conditions and the incident shock speeds measured using five piezoelectric pressure transducers distributed over the final 1.5 m of the driven section. Uncertainty in the experimental pressure and temperature are each less than $\pm 1\%$ [14–16]. The test plane is 2 cm from the end wall of the shock tube with instrument access provided by eight ports. For these experiments, one pair of ports was equipped with ZnSe windows with a 30′ wedge and a broadband anti-reflection (AR) coating providing less than 1% reflection per surface over the wavelength range of 7 to 12 μm. These window characteristics minimize etalon fringe noise when tuning the wavelength of a laser. Another pair of ports was equipped with flat AR-coated ZnSe windows ($R_{avg} < 5\%$ over 8 to 12 μm) for use with fixed wavelength lasers where etalon fringe noise is not a concern. Additionally, one port was instrumented with a transducer to record the pressure in the post-reflected shock region.

Helium and helium-nitrogen driver gas mixtures, as well as driver-section volume inserts, were used to achieve long test times with a steady pressure profile over a broad range of temperature and pressure conditions [17,18]. Test gas mixtures were prepared manometrically in a stainless-steel mixing tank using either neat gases (> 99%) or certified standard gas mixtures (± 2% uncertainty on reported concentration) to supply the target species and high-purity argon (> 99.999%) as a diluent. For the measurements reported here, only dilute test mixtures in argon with a target species concentration no greater than 5% were used in order to limit the endothermic effects of pyrolysis at high temperatures.

2.2. Lasers and optics

Two laser systems were integrated into the shock tube in order to perform absorption cross section measurements using the fractional transmission through the test gas. The fractional transmission is determined by the Beer–Lambert relation:

$$\frac{I}{I_0} = \exp(-\alpha) = \exp(-\sigma n L), \tag{1}$$

where I is the transmitted intensity, I_0 is the incident intensity, α is the absorbance, σ is the absorption cross section in $m^2.mol^{-1}$, n is the number density of the absorbing species in $mol.m^{-3}$, and L is the path length through the gas sample in m.

The first laser system used a Daylight Solutions MIRcat-QT™ with rapid ultra-broad wavelength tuning in order to acquire absorption cross section measurements over a large wavelength range within the test time of the shock tube.

As presented in Fig. 1, the MIRcat-QT™ is outfitted with two external-cavity quantum cascade laser (EC-QCL) modules with wavelength coverage from approximately 8.5 to 10.5 μm (9.6 to 1.78 cm^{-1}) for QCL 1 (M2095-PCX) and approximately 10.5 to 11.7 μm (8.5 to 9.0 cm^{-1}) for QCL 2 (M2115-PC). Variations in the emission intensity are characteristic of the quantum cascade gain medium and are specific to individual lasers. Generally, the emission intensity is strongest in the middle of the coverage region and decreases to zero at the edges. There was approximately a 6 cm^{-1} gap between the spectral coverage offered by these two modules.

The laser modules provided a maximum tuning rate in excess of 30000 $cm^{-1}s^{-1}$ and enabled the full ranges of QCL 1 and QCL 2 to be tuned in less than 10 and 4 ms, respectively. The maximum possible tuning rate was used for all experiments here and only a single laser module was operated during an individual shock tube experiment. With test times ranging from 2 to 8 ms for the temperature and pressure conditions studied in this work, spectral measurements over the full wavelength range of the two module laser system could typically be achieved with two to three repeated experiments.

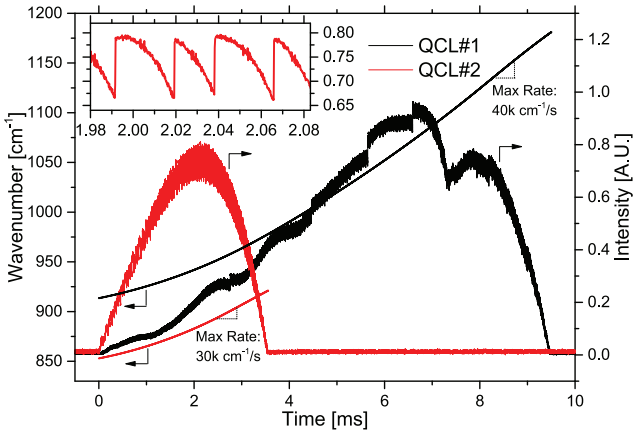

Fig. 1. Wavenumber and intensity tuning characteristics of the Daylight Solutions MIRcat-QT EC-QCL. QCL 1 spans approximately 8.5 to 10.5μm (9.6 to 1.78 cm^{-1}) and QCL 2 spans approximately 10.5 to 11.7 μm (8.5 to 9.0 cm^{-1}).

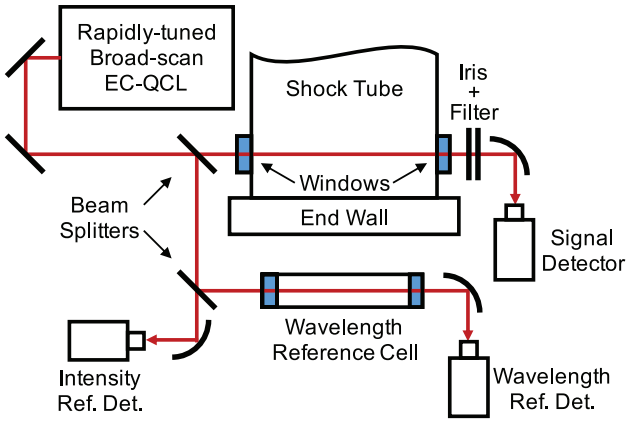

Fig. 2. Schematic of a shock tube configured with a broad-scan rapidly-tuned external-cavity quantum cascade laser. The setup includes an intensity reference detector for common-mode-rejection and a gas-filled wavelength reference cell and detector for wavelength calibration. (Not shown: Fixed-wavelength CO_2 gas laser configured with co-planar alignment.)

A pressure transducer monitoring the passage of the incident shockwave 3.23 m from the shock tube end wall was used to provide the timing signal for the laser system. The rise in the pressure transducer signal was conditioned into a TTL pulse with a variable delay by a pulse/delay generator in order to control the start of the laser scan. The latency between the laser receiving the trigger signal and the start of the laser scan was typically less than 300 ns. The desired start wavelength, end wavelength, and tuning rate for each experiment were configurable in the MIRcat-QT™ control software. The combination of a variable timing delay and selectable start wavelength enabled piece-wise measurement of absorption spectra in cases where the test time was insufficient for the laser to perform a complete scan.

Fig. 1 presents the wavelength-dependent relative intensity for each laser module. The large variation in intensity from the edge to the center of the emission band leads to a corresponding variation in signal-to-noise ratio (SNR). Absorption cross section measurements in regions with insufficient SNR are excluded from the results presented here. This exclusion criteria typically reduced the total tuning range by less than 2%. Repeated experiments with variable gain/attenuation could be used to recover these low SNR regions.

The inset of Fig. 1 presents a detailed view of the laser intensity while rapidly tuning the wavelength. The sawtooth-shaped intensity output is the result of 'micro-hops' in the laser mode as the grating angle is rotated [19]. Instead of continuous wavelength tuning, the laser emits at a steady, fixed wavelength (linewidth: $\leq$0.0033 cm^{-1}) corresponding to the dominant laser mode until it hops in a discrete step ranging in size from approximately 0.2 to 0.6 cm^{-1}. This dominant laser mode is randomly selected from a limited set of candidate modes determined by the combination of the cavity modes (spaced at approximately 0.1 cm^{-1}), the laser gain curve, and the instantaneous grating dispersion curve. As the grating is rotated, the shifting center wavelength of the grating dispersion curve causes the dominant cavity mode to become weaker leading to a drop in intensity until this cavity mode exits the grating dispersion curve. At this moment the laser hops to a new dominant cavity mode, randomly selected among the candidate modes for that grating angle, and the emitted intensity undergoes a sharp step-like rise.

Absorption measurements performed using this form of laser tuning are best interpreted as a sequence of individual narrow-linewidth, fixed-wavelength measurements each with the duration of the corresponding intensity sawtooth. The resulting spectrum comprises discrete absorption cross section values at irregularly spaced wavenumbers. The average spectral interval of the 'micro-hops' (0.35 cm^{-1}) exceeds the laser linewidth by more than a factor of 100, resulting in a highly-resolved but under-sampled spectrum.

As illustrated in Fig. 2, the laser beam was aligned through the shock tube ports equipped with wedged AR-coated ZnSe windows and passed through an iris and long-pass infrared filter before being focussed onto a Vigo Systems™ large-area thermoelectrically-cooled MCT detector (PVM-2TE-10.6). The iris and long-pass infrared filter reduced the quantity of emission from the hot test gas that reached the detector.

Two ZnSe beam splitters were used to direct a fraction of the beam toward both an intensity reference detector and a wavelength reference detector. The intensity reference detector provided a means to perform common-mode noise rejection and thus correct for any laser intensity variations during an experiment. The wavelength reference beam path included a gas cell filled with a mixture of components selected for well-known room-temperature absorption features within the scan range of the laser modules. For the experiments performed here, the mixture was 0.5% ethylene, 0.8% propene, and 2% benzene in a balance of nitrogen at 1 atm. The absorption features produced by this gas mixture provided an absolute wavelength reference for correcting any variations in wavelength tuning performance.

For the second laser system, an Access Laser Company™ CO_2 gas laser was used to measure the absorption cross section at a fixed wavelength and monitor any variations in the concentration of the species of interest during the test time. In the ethylene (C_2H_4) experiments presented here, this laser was operated at the fixed wavelength of 10.532 μm (949.49 cm^{-1}) to probe the peak of the fundamental ν_7 vibrational band (CH_2 wag mode) [20,21]. The beam was aligned through the shock tube ports equipped with flat AR-coated ZnSe windows and focussed onto a Vigo Systems™ MCT detector (PVM-2TE-10.6). The wavelength of the laser was monitored before and after each experiment using a Bristol Instruments™ 771B-XIR spectrum analyzer.

2.3. EC-QCL wavelength calibration

To maintain an accurate wavelength reference for the measured spectra, the EC-QCL wavelength was calibrated relative to the grating-angle at the factory, independently characterized, and then corrected for drift. The factory calibration was reassessed using a spectrum analyzer, the laser output was found to have a

linear relationship of 1.001 cm^{-1}/cm^{-1} (R-squared: 0.9983) and 0.999 cm^{-1}/cm^{-1} (R-squared: 0.9999) between the measured and calibrated wavelengths, respectively for QCL 1 and QCL 2. While the absolute wavelength indicated by the laser was found to drift slightly, the linearity of the relative wavelength was found to be stable.

When tuned rapidly, a wavelength reference pulse was generated every 0.5 cm^{-1} and recorded alongside the detector signals. The fixed-wavelength for each 'micro-hop' was determined by linearly interpolating the wavelength reference pulse signal at the timing of each step-like rise observed in the laser intensity. The average intensity during each individual 'micro-hop' was used in determining the absorbance at the corresponding wavelength.

To assign an absolute wavelength to the measured spectra and correct any drifts in the absolute value of the output wavelength provided by the laser system, a known reference spectrum was measured simultaneously during every shock tube experiment using the configuration detailed in Fig. 2 and Section 2.2. The room-temperature wavelength reference cell provided an absorption spectrum with several strongly absorbing peaks with center wavelengths known to within 0.06 cm^{-1} [10]. To ensure absolute wavelength accuracy in the region of greatest interest, a single prominent reference feature nearest the ethylene band peak was used to assign absolute values to the well-known relative wavelength values during tuning. In the case of QCL 1, the ethylene peak at 949.35 cm^{-1} was used for absolute wavelength correction. For QCL 2, the prominent propene peak at 912.58 cm^{-1} was used. Comparing the resulting calibration to the known locations of other prominent peaks observed in the reference cell mixture of ethylene, propene, and benzene, wavelength discrepancies of less than ± 0.1 cm^{-1} were observed over the range of the scan. To ensure that the accuracy of the measured spectra were not influenced by small absolute wavelength drifts, the above calibration was performed during each shock tube experiment.

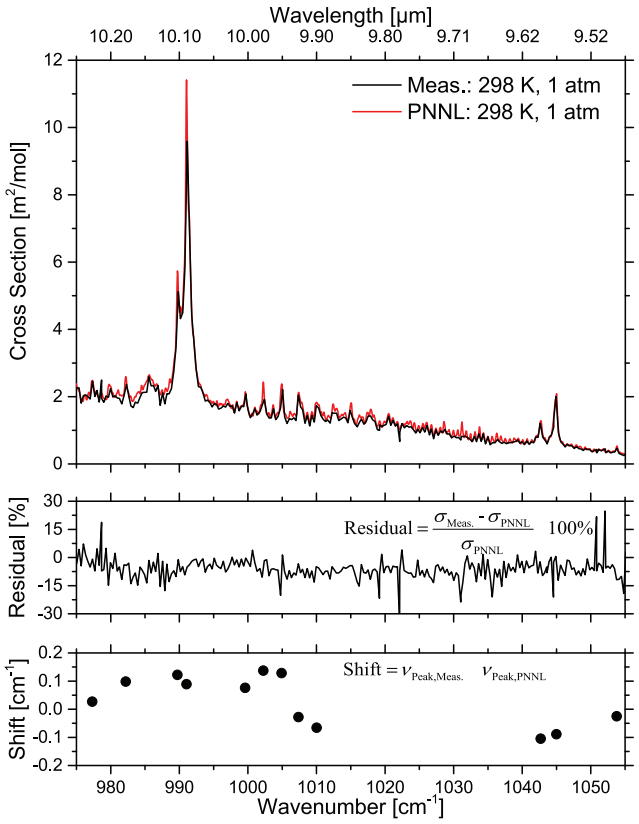

Fig. 3. Comparison of the propene absorption cross section measured at 298 K and 1 atm with the corresponding cross section catalogued in the PNNL Northwest Infrared database [10].

2.4. Absorption cross section and wavelength validation

Validation of the measurement methodology was performed at room temperature and atmospheric pressure where the results may be compared to the PNNL Northwest Infrared database [10]. Fig. 3 presents this comparison for propene. As can be observed, the expected cross section values are faithfully reproduced with residuals not generally exceeding $\pm 10\%$ and major peak locations correctly located within ± 0.15 cm^{-1}. Additionally, the measured integrated cross section over the range of wavelengths in the figure is 5.9% lower than that calculated for the PNNL Northwest Infrared database. These discrepancies are within expectation given that the PNNL reference spectra have a smaller spectral interval of 0.06 cm^{-1} and larger instrument resolution of 0.112 cm^{-1} enabling narrow spectral features to be more reliably captured in comparison to the measured results [10]. At higher temperatures and pressures, line broadening mitigates the need for a smaller spectral interval.

Additional validation of the absorption cross section measured by the EC-QCL was provided during every shock tube experiment by the co-planar CO_2 laser operating at 949.49 cm^{-1}. As demonstrated in Fig. 4, the measured absorbance on both lasers agree at the moment the EC-QCL tunes to the CO_2 laser wavelength.

2.5. Experiment test time

The duration of the test time available for the measurement of absorption cross sections in a shock tube experiment is dependent upon the nominal temperature and pressure conditions as well as the mixture composition. Fig. 4 presents the time-dependent characteristics of a low-temperature and a high-temperature test condition employed in the investigation of the C_2H_4 absorption cross section. For each condition, the pressure time-history measured at the measurement plane is given. Within the test time, the standard deviation of the pressure was observed to be less than 1.5%. A conservative cut-off threshold of 100 μs prior to a pressure change exceeding $\pm 2.5\%$ provides the primary criteria for the end of the test time. For the low-temperature and high-temperature conditions presented here, the test times were 8.6 and 3.0 ms, respectively.

Given the increasing rate of decomposition with temperature for species of interest, deviations in temperature and composition must also be considered when interpreting the measured absorption spectra and defining the serviceable test time. Fig. 4 includes the absorbance time-histories measured by both the scanned-wavelength EC-QCL and the fixed-wavelength CO_2 laser. The fixed-wavelength absorbance measurement allows the target species (C_2H_4) concentration to be monitored throughout the experiment. As illustrated in the figure, at low temperatures the absorbance, and thus concentration, was stable throughout the test time, while at high-temperatures the concentration was rapidly decreasing. For the high-temperature case the absorbance dropped by 50% over the duration of the test time. Decomposition at temperatures appreciably above 1625 K sufficiently curtailed the test time such that measurements were deemed impractical with the presently available wavelength tuning rates.

In addition to decreasing C_2H_4 concentration, this endothermic decomposition caused the gas temperature to decrease. The calculated variations in temperature due to decomposition are also presented in Fig. 4. The time-dependent temperatures for each condition were determined using the ARAMCOMECH 2.0 C_2H_4 mechanism in Chemkin-Pro™ version 17.2 [22]. The calculations as-

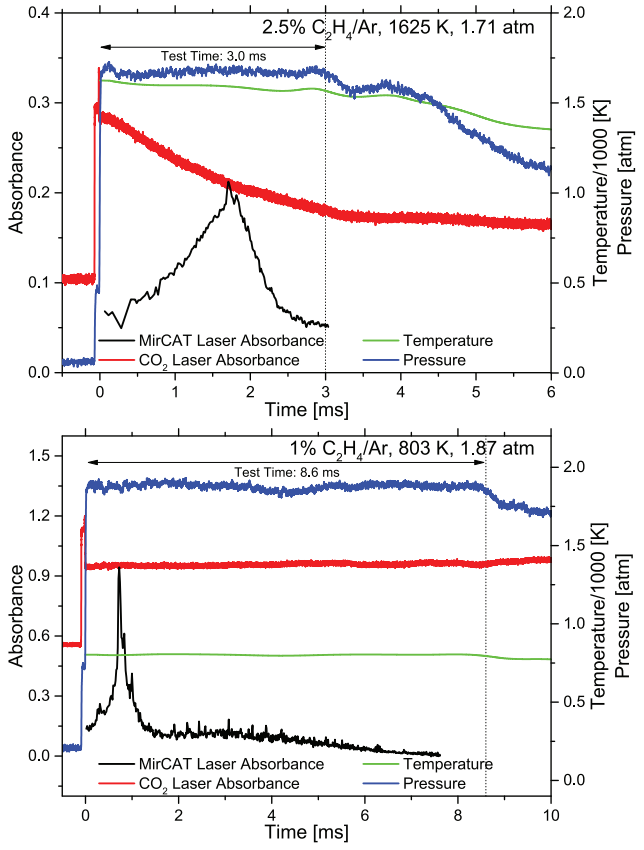

Fig. 4. Absorbance of C_2H_4 as measured by a rapid-tuning EC-QCL during a low-temperature test condition (Bottom: 811 K; 1.91 atm; 1.0% C_2H_4/Ar) and a high-temperature test condition (Top: 1625 K; 1.71 atm; 2.5% C_2H_4/Ar). C_2H_4 absorbance simultaneously measured by a fixed-wavelength CO_2 gas laser at 949.49 cm^{-1} (10.532 μm). Measured pressure time-histories, calculated temperatures time-histories, and serviceable test times are also presented for each shock.

sumed a constant enthalpy reactor with the pressure time-history defined by the measured values. The initial conditions included a temperature determined by frozen-chemistry shock jump relations and a known mixture composition. In the low-temperature condition, where no appreciable decomposition occurs, the temperature is nominally steady. For the high-temperature condition, the temperature dropped 4.1% over the duration of the test time.

The time-dependent concentration and temperature observed during high-temperature experiments influence the absorbance measured by the scanned-wavelength EC-QCL. In the results presented here, the known time-dependent concentration, as measured by the fixed-wavelength CO_2 laser, is used to correct the absorption cross section for the decreasing C_2H_4 concentration. The modeled temperature time-histories and the temperature-dependent absorption cross sections measured by Ren et al. are used to determine the C_2H_4 concentration throughout the test time [21]. The dependence of the absorption cross section on temperature at other measured wavelengths besides 10.532 μm is not independently known and is the subject of this work, thus the scanned-wavelength cross section values reported in figures here are not corrected for variations in temperature but rather the variation in temperature over the duration of the test time is reported alongside each spectra. In the electronic distribution of these results, the corresponding instantaneous temperature (and pressure) are reported for the measured cross section at each individual wavelength that was investigated.

3. High-T and high-P absorption spectra

3.1. Ethylene

C_2H_4 was the first species to be thoroughly investigated using the methodology described above. This species was selected as the initial target based upon favorable spectroscopic and kinetic characteristics, as well as relevance to numerous fields of study.

First, the absorption spectra of C_2H_4 at high temperatures and pressures is sufficiently broadened that the limited spectral interval of the EC-QCL measurements will capture the dominant features. Smaller molecular species may prove to be challenging with this methodology due to narrow spectral features except at very high temperatures and pressures. C_2H_4 is spectroscopically interesting due to the present lack of high-temperature experimental datasets while still being a sufficiently simple molecule that it has been the subject of recent *ab initio* modeling efforts at high-temperatures [12]. The measurements presented here serve to appreciably expand the range of temperatures, pressures, and wavelengths for which quantitative experimental C_2H_4 absorption spectroscopy data is available [10,20,21,23–39].

Next, the comparatively slow decomposition rate of C_2H_4 relative to other larger, less stable molecules allows for longer test times at high-temperatures before the test gas concentration is significantly depleted and the temperature perturbed. The well-studied kinetics of C_2H_4 pyrolysis enable high-confidence in predicting the effects of decomposition on the test gas temperature time-history [22].

Finally, C_2H_4 is relevant to a number of areas of research concerned with high-temperature gases. In high-temperature combustion chemistry C_2H_4 is a key intermediate species from fuel pyrolysis and significantly influences subsequent oxidation chemistry [40,41]. Similarly, C_2H_4 is a pyrolysis product of many modern ablative thermal protection systems for atmospheric entry vehicles and influences boundary layer flow fields, kinetics, and radiation [42–44]. Moreover, C_2H_4 is a constituent of the atmosphere of many substellar objects such as brown dwarfs, gas giants, and super-earths [45,46]. In all of these fields, improved high-temperature C_2H_4 spectroscopic data will enable better diagnostic tools and improved understanding of foundational phenomena.

Fig. 5 presents a comparison of the measured absorption cross section of C_2H_4 at 995 K and 2.28 atm to predictions by HITRAN 2016 and the model by Rey et al. for temperatures up to 700 K [8,12]. The measured spectrum is a concatenation of three shock tube experiments in order to span the full wavelength coverage range of both EC-QCL modules (8.5 to 9.0 cm^{-1}, 9.6 to 1.89 cm^{-1}, and 1.71 to 1.78 cm^{-1}, note the gap in laser coverage near 920 cm^{-1}). The variation in the temperature and pressure of the test conditions for the three experiments was ±5 K and ±0.02 atm, respectively. The results demonstrate the shortcomings of applying a room-temperature database, such as HITRAN 2016, at elevated temperatures. The lack of high-J rovibrational transitions leads to a significant underprediction of the strength and breadth of prominent features. Additionally, new spectral peaks that emerge at high temperatures, such as those neighboring the primary peak near 10.532 μm, are missing from the predicted spectra due to the absence of vibrational hot bands from the database.

The accuracy of the Rey et al. 700K model is considerably better at predicting both the cross section amplitude and the discrete high-temperature features within the spectrum. This database incorporates hot bands and a rotational quantum number cutoff of $J = 71$. This cutoff is sufficient for a fully convergent rotational partition function, and thus a complete line list, for spectrum predictions up to 700 K. However, as stated by Rey et al., a rotational quantum number cutoff of $J = 80 - 85$ would be required for spectrum predictions at 1000 K [12]. The result of the missing lines

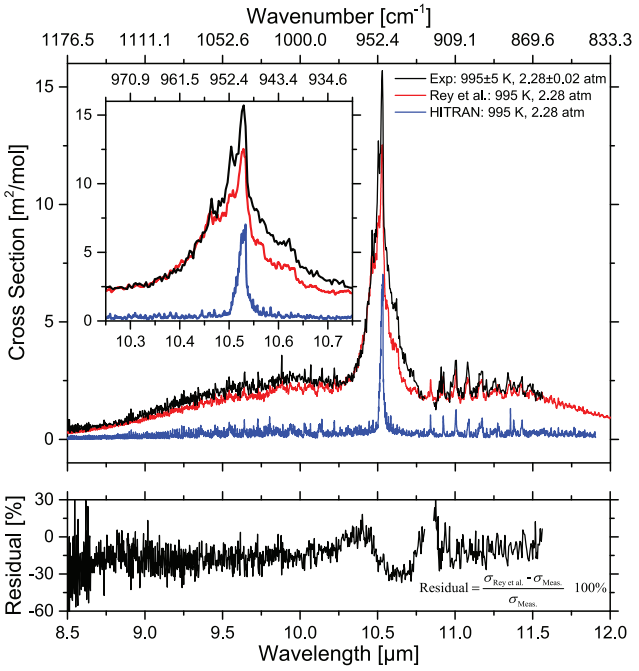

Fig. 5. Comparison of the C_2H_4 absorption cross section measured at 995 K and 2.28 atm with predicted values from HITRAN 2016 and the model by Rey et al. for temperatures up to 700 K [8,12]. The inset provides a detailed view of the ν_7 vibrational band peak near 10.532 μm.

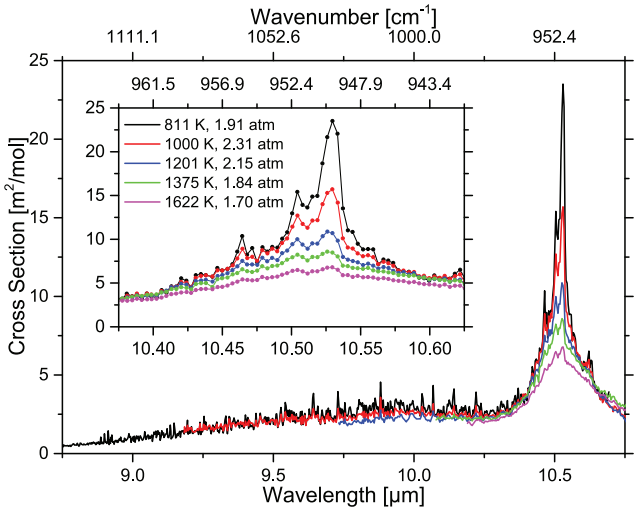

Fig. 6. C_2H_4 absorption cross section measured over a range of temperatures from 8.1 to 1.22 K near 2 atm. The inset provides a detailed view of the ν_7 vibrational band peak near 10.532μm with individual measurement wavelengths indicated by data markers.

with higher rotational numbers presumably bears out in comparisons to the measurements where the residual is observed to be predominantly negative. These missing lines may also account for the observation that the integrated cross section of the model over the measurement wavelength range of 864.9 to 1178.2 cm^{-1} is 13.6% smaller than that of the measurements. Overall, the model is a substantial improvement over those previously available and in this high-temperature case provides predictions with a residual generally less than ±30% relative to the measured cross section.

Measurements of the C_2H_4 absorption cross section were performed at a range of temperatures and pressures presented in Figs. 6 and 7, respectively. The spectra presented in these figures each represent a single shock tube experiment; however, multiple repeated experiments were performed to ensure consistency in the observed spectra. The inset in each figure provides a detailed view of the fundamental ν_7 vibrational band. The data markers within each inset indicate the individual measurement wavelengths and highlight the approximately 0.35 cm^{-1} spectral interval of the measurements.

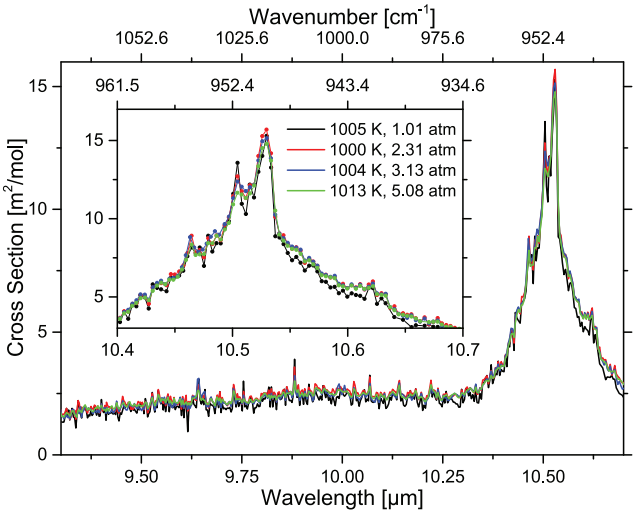

Fig. 7. C_2H_4 absorption cross section measured over a range of pressure from 1.01 to 5.08 atm near 1000 K. The inset provides a detailed view of the ν_7 vibrational band peak near 10.532 μm with individual measurement wavelengths indicated by data markers.

In Fig. 6, five temperatures from 8.1 to 1.22 K were measured near 2 atm. The available test time in a shock tube is inversely related to the test gas temperature. Correspondingly, the available scan range in a single experiment is reduced with increasing temperature. This can be observed in the figure. As discussed in Section 2.5, decomposition is a concern at high temperatures. 1622 K was the only temperature for which appreciable decomposition was observed with a corresponding temperature drop of 4.1% over the duration of the test time. All other conditions experienced minimal decomposition with less than 0.6% temperature drop over the duration of the test time. As expected, significant weakening of the absorption cross section and smoothing of individual features was observed with increasing temperature.

In Fig. 7, four pressures from 1 to 5 atm were measured near 1000 K. These results demonstrate the relative pressure insensitivity of the spectra at high temperatures. Prominent spectral features were smoothed with increasing pressure but the local absorption strength remains largely unchanged. This indicates that small variations in pressure during the shock tube test time or between experiments have little effect on the observed spectra.

3.2. Illustrative spectra

In addition to the measurement of the C_2H_4 absorption cross section at a range of temperatures and pressures, the methodology was applied to several additional species as an illustration of the potential of this approach to generate a new database of high-temperature absorption spectra. Fig. 8 presents measurements of the absorption cross sections of propene (C_3H_6), 1-butene (1-C_4H_8), 2-butene (2-C_4H_8), 1,3-butadiene (1,3-C_4H_6), and methanol (CH_3OH) near 1000 K and 2.3 atm. In general, the current approach may be applied to any infrared-active species under conditions where the salient features may be resolved by the spectral interval of the laser tuning. However, future developments in rapid-tuning, broad-scan laser systems will inevitably reduce the spectral

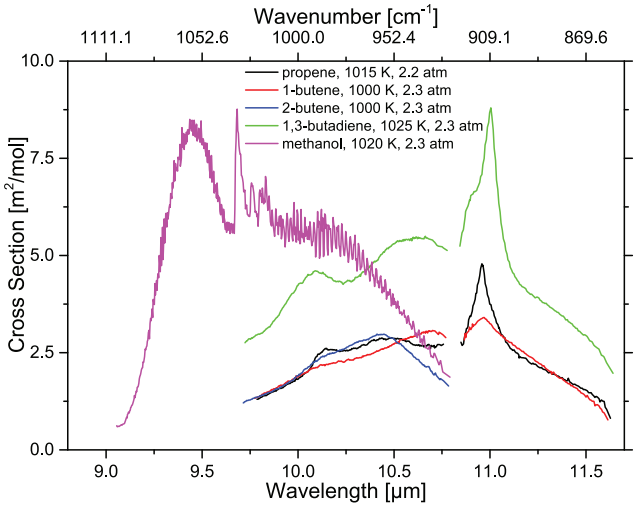

Fig. 8. Absorption cross section measurements for multiple illustrative species (propene, 1-butene, 2-butene, 1,3-butadiene, and methanol) near 1000K and 2.3 atm.

interval, increase the tuning rate, and open new wavelength ranges enabling a greater range of species and conditions.

4. Summary

A methodology has been developed for the measurement of quantitative absorption cross sections for high-temperature and high-pressure gases. The approach leverages the recent development of rapid-tuning, broad-scan EC-QCLs to take advantage of the short-duration near-ideal high-enthalpy test conditions generated by a shock tube test facility.

Absorption cross section measurements of the ν_7 fundamental vibrational band of C_2H_4 from 8.5 to 11.7μm were performed over the temperature range 8.1 to 1.22 K and the pressure range 1 to 5 atm. Additionally, to illustrate the broad range of application, absorption cross section measurements for propene, 1-butene, 2-butene, 1,3-butadiene, and methanol near 1000 K and 2.3 atm were presented.

Using presently available rapid-tuning, broad-scan EC-QCL systems, the methodology is applicable to any infrared-active species with absorption in the wavelength range of approximately 4 to 12μm. This range of wavelengths is rapidly expanding with emerging laser technologies and full coverage of the molecular rovibrational spectrum with broadband, rapid-tuning lasers is anticipated. Shock tubes conceivably permit this methodology to be applied to maximum temperatures and pressures in excess of 10000 K and 1000 atm.

In use, quantitative high-temperature absorption spectra over a wide range of wavelengths could service a need for validation targets in the development of high-temperature empirical and *ab intio* spectral models (emission and absorption). Additionally, the data could be employed in the interpretation of spectroscopic observations and the development of laser absorption spectroscopy sensors.

Overall, the methodology presented here provides an avenue to significantly expand upon existing experimental spectroscopic databases with a new range of previously impractical temperatures and pressures.

Acknowledgements

This material is based upon work supported by, or in part by, the U. S. Army Research Laboratory and the U. S. Army Research Office under contract/grant number W911NF-17-1-0420. Additionally, this work was supported by the Air Force Office of Scientific Research through AFOSR Grant No. FA9550-16-1-0195, with Dr. Chiping Li as contract monitor.

References

[1] Tennyson J, Yurchenko SN, Al-Refaie AF, Barton EJ, Chubb KL, Coles PA, et al. The exomol database: molecular line lists for exoplanet and other hot atmospheres. J Mol Spectrosc 2016;327:73–94. 1603.05890; doi: 10.1016/j.jms.2016.05.002.

[2] Coustenis A, V. Boudon A, Campargue RG, Tyuterev VG. Exo-planetary high-temperature hydrocarbons by emission and absorption spectroscopy (the e-PYTHEAS project). In: Proceedings of the European planetary science congress; vol. 11. 2017.

[3] Rothman L, Gordon I, Barber R, Dothe H, Gamache R, Goldman A, et al. HITEMP, The high-temperature molecular spectroscopic database. J Quant Spectrosc Radiat Transf 2010;111(15):2139–50. doi:10.1016/j.jqsrt.2010.05.001.

[4] Bacsik Z, Mink J, Keresztury G. FTIR Spectroscopy of the atmosphere part 2. Applications. Appl Spectrosc Rev 2005;40(4):327–90. doi:10.1080/05704920500230906.

[5] Francis P, Maciejewski A, Oppenheimer C, Chaffin C. New methods make volcanology research less hazardous. Eos (Washington DC) 1996;77(41):393+396–397.

[6] Goldenstein CS, Spearrin RM, Jeffries JB, Hanson RK. Infrared laser-absorption sensing for combustion gases. Prog Energy Combust Sci 2017;60:132–76. doi:10.1016/j.pecs.2016.12.002.

[7] Hanson RK. Applications of quantitative laser sensors to kinetics, propulsion and practical energy systems. Proc Combust Inst 2011;33(1):1–40. doi:10.1016/j.proci.2010.09.007.

[8] Gordon IE, Rothman LS, Hill C, Kochanov RV, Tan Y, Bernath PF, et al. The HITRAN2016 molecular spectroscopic database. J Quant Spectrosc Radiat Transf 2017;14:0–1. doi:10.1016/j.jqsrt.2017.06.038.

[9] Jacquinet-Husson N, Armante R, Scott NA, Chédin A, Crépeau L, Boutammine C, et al. The 2015 edition of the GEISA spectroscopic database. J Mol Spectrosc 2016;327(June):31–72. doi:10.1016/j.jms.2016.06.007.

[10] Sharpe SW, Johnson TJ, Sams RL, Chu PM, Rhoderick GC, Johnson PA. Gas-phase databases for quantitative infrared spectroscopy. Appl Spectrosc 2004;58(12):1452–61 arXiv:1011.1669v3. doi:10.1366/0003702042641281.

[11] Chu PM, Guenther FR, Rhoderick GC, Lafferty WJ. The NIST quantitative infrared database. J Res Natl Inst Stand Technol 1999;104(1):59–81. doi:10.6028/jres.104.004.

[12] Rey M, Delahaye T, Nikitin AV, Tyuterev VG. First theoretical global line lists of ethylene (12c2h4) spectra for the temperature range 50–700 K in the far-infrared for quantification of absorption and emission in planetary atmospheres. Astron Astrophys 2016;594(A47):1–16.

[13] Tennyson J, Yurchenko SN. Laboratory spectra of hot molecules: data needs for hot super-Earth exoplanets. Mol Astrophys 2017;8:1–18. doi:10.1016/j.molap.2017.05.002.

[14] Oehlschlaeger MA, Davidson DF, Hanson RK. High-temperature thermal decomposition of isobutane and n-butane behind shock waves. J Phys Chem A 2004;108(19):4247–53. doi:10.1021/jp0313627.

[15] Parise TC, Davidson D, Hanson RK. Development of a two-wavelength IR laser absorption diagnostic for propene and ethylene. Meas Sci Technol 2018. doi:10.1088/1361-6501/aab02b.

[16] Farooq A, Jeffries JB, Hanson RK. Sensitive detection of temperature behind reflected shock waves using wavelength modulation spectroscopy of CO_2 near 2.7 μm. Appl Phys B Lasers Opt 2009;96(1):161–73. doi:10.1007/s00340-009-3446-7.

[17] Hong Z, Pang GA, Vasu SS, Davidson DF, Hanson RK. The use of driver inserts to reduce non-ideal pressure variations behind reflected shock waves. Shock Waves 2009;19(2):113–23. doi:10.1007/s00193-009-0205-y.

[18] Hong Z, Davidson DF, Hanson RK. Contact surface tailoring condition for shock tubes with different driver and driven section diameters. Shock Waves 2009;19(4):331–6. doi:10.1007/s00193-009-0212-z.

[19] Buerki P, Weida M. CW Tuning Behavior of CW-PLS Lasers. Technical Report. Daylight Solutions, Inc.; 2008.

[20] Pilla GL, Davidson DF, Hanson RK. Shock tube/laser absorption measurements of ethylene time-histories during ethylene and n-heptane pyrolysis. Proc Combust Inst 2011;33(1):333–40. doi:10.1016/j.proci.2010.06.146.

[21] Ren W, Davidson DF, Hanson RK. IR Laser absorption diagnostic for C2H4 in shock tube kinetics studies. Int J Chem Kinet 2012;44(6):423–32. doi:10.1002/kin.20599.

[22] Metcalfe WK, Burke SM, Ahmed SS, Curran HJ. A hierarchical and comparative kinetic modeling study of C1- C2 hydrocarbon and oxygenated fuels. Int J Chem Kinet 2013;45(10):638–75. doi:10.1002/kin.20802.

[23] Dam N, Engeln R, Reuss J, Pine AS, Fayt A. Ethylene hot bands from molecular jet double-resonance spectroscopy. J Mol Spectrosc 1990;139(1):215–35. doi:10.1016/0022-2852(90)90252-L.

[24] Georges BR, Bach M, Herman M. High resolution FTIR spectroscopy using a slit jet: sa mpling the overtone spectrum of12c2h4. Mol Phys 1997;90(3):381–8. doi:10.1080/002689797172499.

[25] Sartakov BG, Oomens J, Reuss J, Fayt A. Interaction of vibrational fundamental and combination states of ethylene in the 3 μm region. J Mol Spectrosc 1997;185(1):31–47. doi:10.1006/jmsp.1997.7378.

[26] Bach M, Georges R, Hepp M, Herman M. Slit-jet fourier transform infrared spectroscopy in 12c2h4: cold and hot bands near 3000 cm. Chem Phys Lett 1998;294(6):533–7. https://doi.org/10.1016/S0009-2614(98)00889-6.
[27] Bach M, Georges R, Herman M, Perrin A. Investigation of the fine structure in overtone absorption bands of 12c2h4. Mol Phys 1999;97(1–2):265–77. doi:10.1080/00268979909482828.
[28] Blass WE, Hillman JJ, Fayt A, Daunt SJ, Senesac LR, Ewing AC, et al. 10 µm ethylene: spectroscopy, intensities and a planetary modeler's atlas. J Quant Spectrosc Radiat Transf 2001;71(1):47–60. doi:10.1016/S0022-4073(01)00011-5.
[29] Blanquet G, Bouanich JP, Walrand J, Lepère M. Diode-laser measurements and calculations of N2-broadening coefficients in the $\nu 7$ band of ethylene. J Mol Spectrosc 2005;229(2):198–206. doi:10.1016/j.jms.2004.09.004.
[30] Rotger M, Boudon V, Vander Auwera J. Line positions and intensities in the $\nu 12$ band of ethylene near 1450 cm- 1: an experimental and theoretical study. J Quant Spectrosc Radiat Transf 2008;109(6):952–62. doi:10.1016/j.jqsrt.2007.12.005.
[31] Ulenikov ON, Onopenko GA, Bekhtereva ES, Petrova TM, Solodov AM, Solodov AA. High resolution study of the $\nu 5 + \nu 12$ band of C2H4. Mol Phys 2010;108(5):637–47. doi:10.1080/00268971003645362.
[32] Loroño Gonzalez MA, Boudon V, Loëte M, Rotger M, Bourgeois MT, Didriche K, et al. High-resolution spectroscopy and preliminary global analysis of C-H stretching vibrations of C2H4 in the 3000 and 6000cm-1 regions. J Quant Spectrosc Radiat Transf 2010;111(15):2265–78. doi:10.1016/j.jqsrt.2010.04.010.
[33] Flaud JM, Lafferty WJ, Sams R, Malathy Devi V. High resolution analysis of the ethylene-1-13c spectrum in the 8.4–14.3 µm region. J Mol Spectrosc 2010;259(1):39–45. doi:10.1016/j.jms.2009.10.003.
[34] Flaud JM, Lafferty WJ, Malathy Devi V, Sams RL, Chris Benner D. Absolute line intensities and self-broadened half-width coefficients in the ethylene-1-13c bands in the 700–1190 cm-1 region. J Mol Spectrosc 2011;267(1–2):3–12. doi:10.1016/j.jms.2011.01.002.
[35] Lafferty WJ, Flaud J, Tchana FK. The high-resolution infrared spectrum of ethylene in the 1800 - 2350 cm spectral region. Mol Phys 2011;109(21):2501–10. doi:10.1080/00268976.2011.577040.
[36] Lebron GB, Tan TL. Integrated band intensities of ethylene (12c2h4) by fourier transform infrared spectroscopy. Int J Spectrosc 2012;2012:1–5. doi:10.1155/2012/474639.
[37] Ben Hassen A, Kwabia Tchana F, Flaud JM, Lafferty WJ, Landsheere X, Aroui H. Absolute line intensities for ethylene from 1800 to 2350 cm-1. J Mol Spectrosc 2012;282(1):30–3. doi:10.1016/j.jms.2012.11.001.
[38] Alrefae M, Es-Sebbar ET, Farooq A. Absorption cross-section measurements of methane, ethane, ethylene and methanol at high temperatures. J Mol Spectrosc 2014;303:8–14. doi:10.1016/j.jms.2014.06.007.
[39] Vander Auwera J, Fayt A, Tudorie M, Rotger M, Boudon V, Franco B, et al. Self-broadening coefficients and improved line intensities for the $\nu 7$ band of ethylene near 10.5 µm, and impact on ethylene retrievals from jungfraujoch solar spectra. J Quant Spectrosc Radiat Transf 2014;148:177–85. doi:10.1016/j.jqsrt.2014.07.003.
[40] Xu R, Chen D, Wang K, Tao Y, Shao JK, Parise T, et al. Hychem model: application to petroleum-derived jet fuels. 10th US Natl Combust Meet 2017:1–6.
[41] Xu R, Wang H, Davidson DF, Hanson RK, Bowman CT, Egolfopoulos FN. Evidence supporting a simplified approach to modeling high-temperature combustion chemistry. Proceedings of the 10th US National Combustion Meeting 2017b;:1–6.
[42] Lincoln KA. Experimental determination of vapor species from laser-Ablated carbon phenolic composites. AIAA 1983;21(8):1204–7. doi:10.2514/3.8227.
[43] Martin A, Boyd I, Cozmuta I, Wright M. Chemistry model for ablating carbon-Phenolic material during atmospheric re-Entry. Proceedings of the 48th AIAA aerospace sciences meeting including the new horizons forum and aerospace exposition2010;(January). doi:10.2514/6.2010-1175.
[44] Helber B, Chazot O, Magin T, Hubin A. Space and time-Resolved emission spectroscopy of carbon phenolic ablation in air and nitrogen plasmas. Proceedings of the 44th AIAA Thermophysics Conference2013;:1–14. doi:10.2514/6.2013-2770.
[45] Lodders K, Fegley B. Atmospheric chemistry in giant planets, brown dwarfs, and low-mass dwarf stars. i. carbon, nitrogen, and oxygen. Icarus 2002;155(2):393–424. doi:10.1006/icar.2001.6740.
[46] Hu R, Seager S. Photochemistry in terrestrial exoplanet atmospheres. III. photochemistry and thermochemistry in thick atmospheres on super earths and mini neptunes. Astrophys J 2014;784(1) 1401.0948. doi:10.1088/0004-637X/784/1/63.